ISSN: 2469-5866

Tahriri. Int J Brain Disord Treat 2024, 10:052
DOI: 10.23937/2469-5866/1410052
Volume 10 | Issue 1
Open Access

International Journal of
Brain Disorders and Treatment

REVIEW ARTICLE

Harnessing Magnetic Resonance-Guided Focused Ultrasound for Precise Blood-Brain Barrier Disruption: Advancements in Targeted Therapeutics for Neurological Disorders

Mohammadreza Tahriri*

Department of Engineering, Norfolk State University, Norfolk, VA, USA

***Corresponding author:** *Mohammadreza Tahriri, Department of Engineering, Norfolk State University, Norfolk, VA, USA*

Abstract

This review examines the latest advancements in the clinical application of Magnetic Resonance-guided Focused Ultrasound (MRgFUS), also referred to as Magnetic Resonance High-Intensity Focused Ultrasound (MR-HIFUS), for transiently permeabilizing the blood-brain barrier (BBB), thereby enhancing drug delivery for neurological disorders treatments. Extensive preclinical studies and human safety trials have established a robust safety profile for MRgFUS, supporting its use in conditions such as Alzheimer's disease, Parkinson's disease, and brain tumors. By disrupting the BBB, MRgFUS facilitates the targeted delivery of systemic medications to specific brain regions, significantly improving therapeutic efficacy. This technique has shown promise in increasing the concentration of antitumor agents, including chemotherapy, immunotherapy, and gene therapy, in brain tumors, thus prolonging survival and delaying disease progression in animal models. Additionally, combining MRgFUS with advanced drug delivery systems such as liposomes, modified microbubbles, and magnetic nanoparticles has been found to enhance drug penetration and reduce treatment toxicity. This review highlights the potential of MRgFUS in transforming the treatment of neurological disorders by optimizing drug delivery and minimizing adverse effects on healthy brain tissue.

Keywords

MRI, Focused ultrasound, MRgFUS, BBB, Neurological disorders, Drug delivery

Introduction

The BBB serves as a selective barrier between the bloodstream and the central nervous system (CNS), composed of tightly joined endothelial cells and efflux transporters. This barrier permits the passage of ions and small lipid-soluble molecules under 400 Da while restricting larger molecules [1,2]. The BBB is crucial for maintaining a stable CNS environment, safeguarding it from potentially harmful substances, but it also poses a significant challenge for delivering therapeutic agents to the brain [3,4]. Various strategies to enhance BBB permeability are being explored, broadly classified into transcellular and paracellular methods [5]. Transcellular techniques involve increasing the lipophilicity of molecules or utilizing carrier-mediated transport to facilitate BBB crossing [6]. However, these methods are constrained by the pharmacological properties of the agents. Paracellular strategies involve the temporary disruption of tight junctions, using either chemical agents like hyperosmolar compounds or physical methods such as ultrasound, which can transiently open the BBB [5].

Among the paracellular approaches, the use of low-intensity ultrasound combined with microbubble injection has gained prominence. This method allows for targeted, reversible BBB opening in specific brain regions, demonstrated in various preclinical models [7]. Clinical trials utilizing MRgFUS, also known as MR-HIFUS, have demonstrated promising outcomes, showcasing their efficacy and safety in permeabilizing the BBB. This technique employs an MRI-compatible helmet with focused ultrasound transducers, providing real-time imaging guidance and allowing for the monitoring of BBB disruption via gadolinium (Gd) contrast [1]. MRgFUS is particularly beneficial in treating movement disorders and certain psychiatric conditions, with potential applications

Citation: Tahriri M (2024) Harnessing Magnetic Resonance-Guided Focused Ultrasound for Precise Blood-Brain Barrier Disruption: Advancements in Targeted Therapeutics for Neurological Disorders. Int J Brain Disord Treat 10:052. doi.org/10.23937/2469-5866/1410052

Accepted: September 26, 2024: **Published:** September 28, 2024

in neuromodulation when used at lower intensities [8-11]. Additionally, devices like SonoCloud offer a more continuous method of BBB disruption, suitable for treatments requiring repeated sessions [12,13].

The blood-tumor barrier (BTB) presents an additional challenge and opportunity for targeted drug delivery. As brain tumors grow, they disrupt the normal architecture of the BBB, forming the BTB, which is characterized by increased permeability [14,15]. However, this disruption is often insufficient for therapeutic concentrations of drugs to reach the tumor site without affecting the surrounding healthy brain tissue. MRgFUS offers a promising method for enhancing drug delivery across the BTB by transiently increasing its permeability, thereby improving the localization of chemotherapeutic agents and minimizing systemic toxicity [14,16].

Following BBB and BTB opening, systemic administration of drugs can achieve targeted delivery to the CNS, including small molecules, monoclonal antibodies, and even neural stem cells [17]. This approach is under investigation for various conditions, including Alzheimer's disease, Parkinson's disease, and brain tumors [18,19]. The efficacy of MRgFUS in enhancing the delivery of chemotherapeutic agents has been demonstrated, showing significantly higher concentrations in the brain tissue with reduced systemic toxicity [16]. This review focuses on the latest advancements in ultrasound-mediated BBB and BTB permeabilization techniques, emphasizing their potential for safe, targeted, and effective drug delivery in the treatment of Neurological disorders.

Mechanisms and Techniques in MRgFUS

High-intensity focused ultrasound

High-intensity focused ultrasound (HIFUS) is an innovative noninvasive method that offers an alternative to traditional hyperthermia techniques. It works by concentrating ultrasonic waves from an external transducer to raise the temperature in specific tissues, providing targeted thermal effects. This technique is particularly beneficial as it can be precisely directed to deep tissues within the body, achieving both mild and ablative hyperthermia. The interaction between ultrasound waves and tissue can produce thermal and mechanical bioeffects, enhancing drug extravasation, uptake, and release from temperature-sensitive or pressure-sensitive drug delivery systems [20-22].

These bioeffects can also improve intracellular drug delivery and increase tissue permeability [23]. The parameters of HIFUS, such as power, frequency, duty cycle, and timing, can be adjusted to fine-tune and control these bioeffects. When combined with MRI for guidance, known as MRgFUS or MR-HIFUS, this technique allows for high-resolution anatomical imaging and precise monitoring of temperature changes and tissue displacement during therapy.

MR-HIFUS has been extensively used for the ablation of symptomatic uterine leiomyomata [24,25]. Its application is expanding into various oncological treatments, including benign breast fibroadenomas [26], malignant breast carcinoma [27], prostate cancer [28], palliative care for painful bone metastases [29], and brain tumor ablation [30]. Additionally, MRgFUS/MR-HIFUS is being explored for treating neurological disorders such as epilepsy, essential tremor, neuropathic pain, and Parkinson's disease [31-33]. It also shows potential as an immunomodulatory tool to prevent local tumor recurrence and metastasis post-ablation [34]. Moreover, MRgFUS/MR-HIFUS has demonstrated effectiveness in enhancing drug delivery to the brain by modulating the BBB [35].

Principles of focused ultrasound

Ultrasound is a type of mechanical wave that travels through a medium at frequencies higher than the human audible range of 20 Hz [36]. When ultrasound waves encounter a boundary between two media with different acoustic impedances, phenomena such as reflection and refraction occur [37]. Specular reflection, which happens when ultrasound waves hit a smooth surface, helps delineate interfaces between soft tissues, thereby providing clear images of organ boundaries for diagnostic purposes [38,39]. Additionally, ultrasound waves experience attenuation due to absorption and scattering, which can convert acoustic energy into heat. This thermal effect can lead to protein denaturation, coagulation, cell necrosis, and ultimately, tissue ablation [30,40,41]. Ultrasound can also induce cavitation, a process where microbubbles form and oscillate, potentially causing mechanical damage to tissues through high-pressure and shear forces [42,43].

The development of FUS technology began with Gruetzmacher's design of a curved quartz plate to focus ultrasound beams at a specific point in 1935 [44]. Since then, advances in phased array transducers, comprising hundreds of piezoelectric elements, have significantly improved FUS's ability to navigate complex tissue structures, such as bone, and to focus on multiple points simultaneously, enhancing the therapeutic volume [45,46]. Modern systems allow clinicians to adjust sonication parameters, including acoustic energy intensity, frequency, and duration, tailored to the treatment's objectives and patient characteristics.

The thermal and mechanical effects of ultrasound underpin its therapeutic applications in clinical settings, particularly in stereotactic ablative surgery. This technique, known as MRgFUS, offers a non-invasive alternative to traditional thermal therapies like radiofrequency (RF) ablation. Furthermore, under specific sonication conditions, cavitation effects can selectively and reversibly open the BBB, which is being actively investigated for its potential in enhancing drug delivery to the brain and neuromodulation [10,47,48].

MRgFUS BBB opening procedure

The MRgFUS BBB opening procedure utilizes the 220 kHz ExAblate Neuro 4000 system, featuring 1024 ultrasound transducers integrated with a 3T MRI scanner. Initially, the subject's hair is shaved closely to the scalp, and a Cosman-Roberts-Wells stereotactic frame is applied under local anesthesia for precise alignment. The subject is positioned supine on the MRI table, equipped with compression stockings, and all pressure points are carefully padded. The frame is then secured to the ExAblate helmet, with degassed water acting as a medium between the scalp and transducers to ensure optimal contact. Vital signs and electrocardiogram are continuously monitored using MR-compatible, non-invasive systems throughout the procedure. Participants remain comfortable and alert, with the ability to halt the procedure if they experience discomfort or an emergency [36,49].

The procedure commences with the acquisition of planning MR images, registered with baseline scans for accurate targeting. The focus is on opening the BBB in specific regions of the body, such as the arm or leg. Two targets are identified in these regions, each carefully chosen to avoid critical areas and minimize the risk of adverse effects. Within these targets, the focused ultrasound beam is precisely guided to ensure effective and safe BBB opening, following a predetermined pattern to maximize coverage while minimizing risk.

For transcranial focused ultrasound procedures targeting the BBB, estimating *in vivo* tissue pressure for individual patients is complicated by variations in skull shape, density, and the specific locations targeted. To address this, the optimal power level for BBB opening is established using cavitation feedback through a process known as a ramp test. This technique involves gradually increasing the power in small increments, usually around 5%, during brief sonications. The device's hydrophones monitor for sub-harmonic acoustic signals from the target area, which indicate the onset of cavitation. Once detected, the optimal power for opening the BBB is determined to be approximately 50% of this cavitation threshold, ensuring effective treatment while reducing the risk of side effects.

The procedure includes administering one to two 90-second ultrasound cycles to achieve the desired effect, accompanied by the intravenous injection of microbubbles. The dose of microbubbles is carefully controlled to not exceed a specific limit. Ultrasound is applied in burst mode with specific parameters, including a pulse repetition period and duty cycle, targeting multiple areas.

During the procedure, real-time monitoring includes acoustic monitoring, MRI thermometry, and direct feedback from the patient. MRI thermometry is performed using a standard fast spoiled gradient echo (FSPGR) sequence, ensuring no interference with the cavitation receivers in the focused ultrasound array. After each ultrasound cycle, patients undergo clinical and radiological assessments to check for adverse events, using Gd-enhanced T1-weighted and gradient echo (GRE) sequences to evaluate BBB permeability, tissue integrity, and the presence of microhemorrhages. The appearance of new Gd enhancement in the targeted brain area indicates successful BBB opening, at which point the procedure is concluded. Clinical and MRI assessments are conducted the following day to evaluate the reversibility of BBB opening and any adverse events [49].

Mechanism of BBB disruption using ultrasound

Microbubbles, which are small gas-filled spheres with a microsphere shell, are introduced into the bloodstream peripherally. Initially designed as a contrast agent for cardiac ultrasound diagnostics, microbubbles are now used for opening the BBB via ultrasound [1,50]. When microbubbles are exposed to ultrasound in targeted brain regions, as precisely defined by patient-specific MRI, they oscillate, causing a temporary disruption of the BBB (Figure 1). The degree of BBB disruption depends on factors such as acoustic pressure, duration of sonication, and microbubble size [51,52]. Excessive oscillation forces can, however, lead to hemorrhage. These forces induce stretching, acoustic streaming, and shear stress on blood vessels, impacting the permeability of tight junctions and the activity of efflux transporter proteins [48,53].

There are various microbubble formulations available, with the ideal type promoting stable cavitation, reducing P-glycoprotein production nearby, and facilitating caveolae formation (membrane invaginations) [54,55]. A study evaluating three different commercial microbubble products found them equally effective in terms of the extent and duration of BBB permeability [56]. The performance of microbubbles can be optimized by adjusting ultrasound parameters such as power and duration based on the microbubble's size and half-life [56].

Early preclinical research was crucial in establishing safe parameters for FUS. These studies indicated that using lower frequencies and peak pressures is consistently safe, promoting harmonic bubble oscillations instead of bubble collapse, thereby preventing damage to blood vessels, neurons, or glial cells [57]. A mechanical index (MI), calculated as the peak negative pressure (estimated *in situ*) divided by the square root of the ultrasound frequency, was developed, with an MI ≤ 0.45 being consistently safe and not associated with hemorrhage [58].

The process of BBB permeability is dynamic, occurring almost immediately after the ultrasound sonication of microbubbles. Confirmation of BBB closure can be

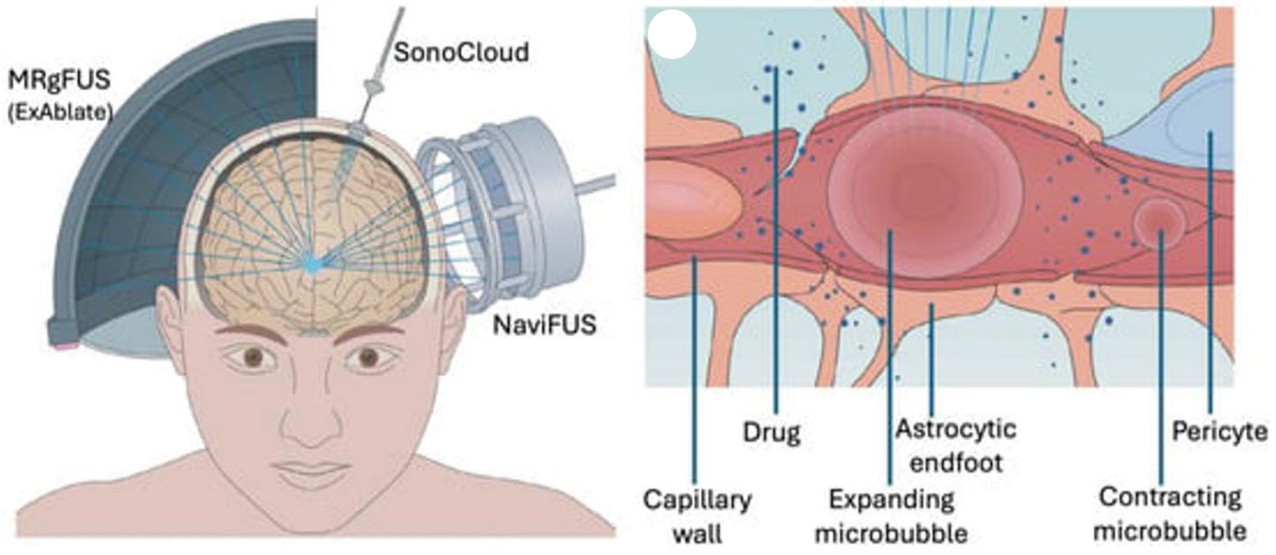

Figure 1: Mechanisms and systems of ultrasound-mediated drug delivery. Illustrated are three different systems: The ExAblate system, which includes a helmet with a phased array of ultrasound transducers, separated from the scalp by cooled degassed water and operated within an MRI environment. The SonoCloud system involves an implanted device placed through a burr hole in the skull, either during a tumor resection surgery or as a separate procedure, powered by a transdermal needle connected to an external power supply for each treatment session. The NaviFUS system is similar to the ExAblate, featuring a multi-channel array with a smaller surface area, but it does not operate within an MRI. The interaction of microbubbles with sonicated tissue causes cavitation, which exerts mechanical forces on the capillary walls, astrocytic endfeet, and pericytes, temporarily opening the blood-brain barrier to allow the passage of larger molecules into the brain parenchyma [1].

achieved via histology and non-invasive imaging, such as MRI, typically within 3-24 hours [35,59]. T1-weighted MRI with gadolinium contrast is commonly used to demonstrate BBB opening and subsequent restoration. Initial human trials focused on a small tissue volume (1 cm^3) per treatment, but recent studies have safely increased this to 40 cm^3 with repeated sessions [60], with even larger volumes being tested in non-human primates [61].

Alternative strategies using ultrasound to enhance drug delivery are also under active investigation. One such approach involves nanodroplets, which have a longer half-life than microbubbles and can carry therapeutic agents. These nanodroplets can be administered systemically and, upon reaching the ultrasound target area, vaporize to release the drug locally [62]. This technique has been used, for instance, to deliver phenobarbital to the amygdala for treating agitation in an Alzheimer's disease mouse model [63]. Another innovative method involves administering a piezoelectric nanogenerator to rodents, which embeds into neuronal membranes. When activated by FUS, this device stimulates tyrosine hydroxylase activity, enhancing dopamine production in striatal neurons [64]. While nanodroplets and nanogenerators hold great potential for future innovations, the established safety and reliability of transcranial and implantable FUS devices for BBB opening have already led to several completed and ongoing translational human clinical trials [1] (Figure 1).

Advanced Techniques in Image-Guided Drug Delivery

In the context of personalized medicine, achieving the "right treatment for the right patient at the right time" is a fundamental principle. To achieve this, innovative tools are necessary to tailor therapies to individual patient needs. Image-guided drug delivery (IGDD) has emerged as a promising approach, utilizing clinical imaging techniques to enhance the precision of drug delivery systems. This method involves the use of imaging to delineate target and non-target areas, as well as for screening, treatment planning, monitoring, and post-treatment evaluation [65].

MR-guided drug delivery

MR imaging is particularly advantageous in IGDD due to its capacity for high spatial and temporal resolution imaging and quantitative assessments during therapeutic interventions. MR-guided drug delivery not only complements existing minimally invasive therapies but also holds the potential to improve their efficacy and broaden their clinical applications. This review delves into the current advancements in MR-guided drug delivery, with an emphasis on hyperthermia-mediated delivery techniques and prospective future developments in this field [65].

MR imaging offers distinct advantages over other imaging modalities like ultrasonography and computed tomography, making it particularly suitable for guiding

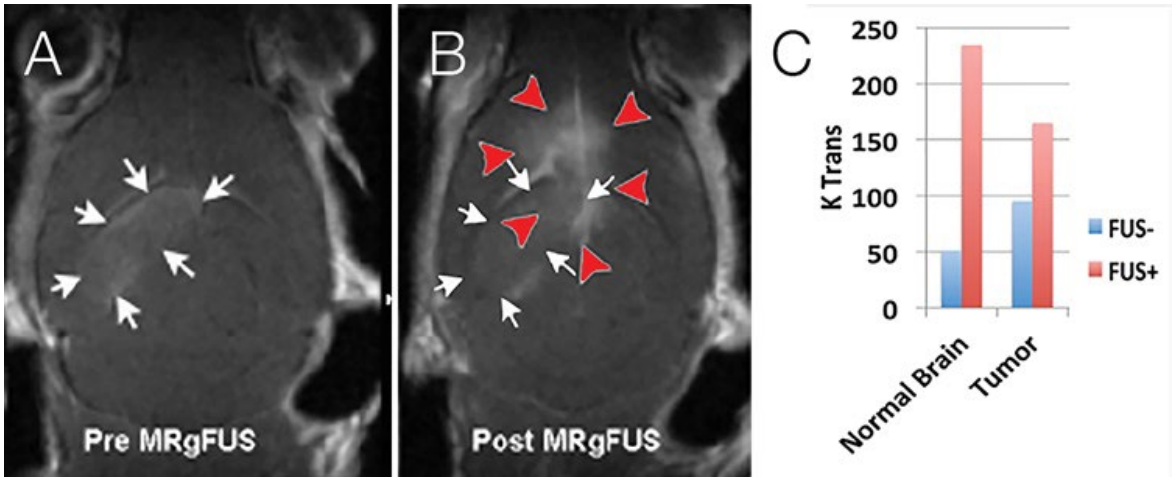

Figure 2: (A and B) T1-weighted MRI images with post-gadolinium enhancement in a mouse brain, highlighting a tumor in the right hemisphere (indicated by arrows). Image A shows the tumor before the application of MRgFUS, while image B displays increased enhancement (marked by arrowheads) in both the tumor and surrounding normal tissue due to the opening of the blood-brain barrier (BBB) post-treatment; C) Prior to MRgFUS (FUS-), the volume transfer constant (Ktrans) from dynamic contrast-enhanced imaging was higher in the tumor compared to normal brain tissue. Following MRgFUS (FUS+), an increase in BBB permeability was observed in both normal and tumor tissues [14].

drug delivery. One key advantage is its ability to provide excellent contrast between soft tissues and between normal and abnormal structures, owing to tissue-specific MR parameters. This high level of contrast enhances the precision of treatment planning. Importantly, MR imaging does not involve ionizing radiation, which is crucial for procedures requiring repeated imaging to monitor drug delivery and assess tumor progression [65].

Additionally, MR imaging offers comprehensive anatomical, functional, and metabolic data through volumetric and multiplanar imaging techniques. This multifaceted capability has been increasingly employed in the planning, monitoring, and post-treatment assessment of drug delivery systems, particularly when used in conjunction with HIFUS [66].

Clinical Applications of MRgFUS in Neurological Disorders

Brain tumor management with MRgFUS

The utilization of MRgFUS and microbubbles has shown promise in overcoming the BBB and BTB for the enhanced delivery of chemotherapeutics. In a rat brain glioma model, MRgFUS significantly increased the concentration of doxorubicin (DOX) in gliomas, achieving levels over 2.5 times higher than control tumors at one-hour post-treatment, and nearly 14 times higher at 24 hours [14,67]. This effect suggests that MRgFUS not only facilitates drug delivery but also prolongs the duration of drug concentration in the target area. However, the response of the BBB and BTB to MRgFUS can vary depending on the systemic treatment used. For instance, while MRgFUS improved BCNU delivery to normal brain tissue by 340%, the increase was only 202% in tumor-bearing rats ($p < 0.05$) [68], indicating a possible treatment-dependent variation in BTB disruption. These findings are supported by unpublished experimental data in tumor-implanted mice (Figure 2).

The application of MRgFUS can significantly enhance the penetration of chemotherapeutic drugs through the BTB, thereby improving treatment efficacy and survival outcomes in tumor models. For instance, in a rat glioma model, combining MRgFUS with systemic carmustine (BCNU) administration resulted in a notable increase in median survival time compared to untreated controls (53 days *vs*. 29 days) and those receiving BCNU alone (53 days *vs*. 32 days, with no reported significance) [68]. This suggests that MRgFUS enhances the effectiveness of chemotherapy, as it did not provide survival benefits on its own. In a similar study, the combination of temozolomide (TMZ) and MRgFUS in rats significantly extended median survival compared to no treatment (23 days *vs*. 20 days), whereas TMZ alone did not show a significant difference compared to the untreated group (21 days *vs*. 20 days) [69]. Additionally, the use of MRgFUS with TMZ significantly reduced tumor growth compared to TMZ alone, with tumors growing 21 times their original size without MRgFUS and only 5 times with MRgFUS over a one-week period. These findings indicate that MRgFUS not only improves the delivery of systemic chemotherapy but also enhances its overall efficacy, although further research is needed to fully understand the dose-response relationship.

Nanoparticles provide an alternative to liposomal encapsulation, which may cause potential side effects [70]. Magnetic nanoparticles offer a promising synergy with MRgFUS for drug delivery. These magnetic nanoparticles can be linked to chemotherapeutics and directed to specific areas using an external magnetic field, a technique known as magnetic targeting [71].

Additionally, magnetic nanoparticles serve as contrast agents, potentially eliminating the need for gadolinium in MRgFUS treatments [72]. While magnetic nanoparticles typically struggle to cross the BBB, their accumulation in brain tissue can be significantly enhanced when combined with MRgFUS [73]. This process involves an "open-then-pull" method, where MRgFUS first disrupts the BBB, allowing circulating MNPs to be attracted to the permeabilized area by a magnetic field.

Early animal studies have demonstrated the potential of combining magnetic nanoparticles with MRgFUS to enhance treatment delivery to brain tumors. For example, in a rat glioma model treated with epirubicin-conjugated magnetic nanoparticles, MRgFUS, and magnetic targeting, there was a 2.4-fold increase in magnetic nanoparticle accumulation in the targeted hemisphere compared to the opposite hemisphere, whereas the combination of magnetic nanoparticles and MRgFUS without magnetic targeting resulted in only a 1.2-fold increase [73]. This enhanced accumulation led to a 16-fold increase in epirubicin concentration in brain tissue treated with MRgFUS and MT compared to MRgFUS alone. Additionally, the group receiving magnetic nanoparticles MRgFUS, and magnetic targeting showed prolonged survival compared to untreated controls (31 days *vs*. 18 days) or those treated with magnetic nanoparticles and MRgFUS without magnetic targeting (30.5 days *vs*. 20 days). Tumor growth was also significantly delayed in the MRgFUS and MT group compared to untreated controls over seven days (106% ± 24% vs. 313% ± 103%). The study noted that to apply magnetic targeting in humans, due to anatomical differences, a superconducting magnetic coil or more strongly magnetic nanoparticles might be necessary [73]. Similar findings were observed with BCNU [74]. Both MRgFUS alone and magnetic targeting alone doubled magnetic nanoparticle concentration in the treated brain regions compared to untreated regions, while the combination of magnetic nanoparticles, MRgFUS, and magnetic targeting increased magnetic nanoparticles accumulation by nearly 10-fold compared to untreated regions and 26-fold compared to magnetic nanoparticles without additional treatment. A week after treatment, the medium-dose magnetic nanoparticles, MRgFUS, and magnetic targeting group showed significantly delayed tumor progression compared to no treatment (-0.79 ± 0.35 cm^3 vs. 2.98 ± 2.61 cm^3) or magnetic nnaoparticles alone (-0.79 ± 0.35 cm^3 *vs*. 2.96 ± 3.00 cm^3). Furthermore, magnetic nanoparticles alone were more effective than unbound BCNU (1.15 ± 1.58 cm^3 vs. 2.48 ± 3.09 cm^3), with the effect being dose-dependent [74].

To simplify protocols involving magnetic nanoparticles, researchers have developed microbubbles conjugated with superparamagnetic iron oxide nanoparticles (SPIONs), a type of magnetic nanoparticles, loaded with DOX [75]. This single formulation combines the functions of microbubbles, gadolinium contrast, and chemotherapy-conjugated magnetic nanoparticles, enhanced by MRgFUS and magnetic targeting. In a rat glioma model, SPION deposition increased fourfold with MRgFUS and magnetic targeting compared to the non-targeted hemisphere, while MRgFUS alone and magnetic targeting alone resulted in 2.7-fold and 2.3-fold increases, respectively. Additionally, DOX deposition in the treated hemisphere increased twofold with MRgFUS and magnetic targeting compared to the control. A follow-up study using an improved formulation that enhanced DOX-carrying capacity and R2 relaxivity demonstrated that SPION-DOX complexes accumulated 2.8 times more in MRgFUS-targeted brain tissue with MT compared to without magnetic targeting. DOX deposition was also enhanced by more than 2.1 times with magnetic targeting. The MR R2 value was highly correlated with SPION concentration (R^2 = 0.83) and DOX accumulation (R^2 = 0.79), suggesting that SPION-DOX microbubbles may be advantageous for dosing monitoring through imaging [75].

Advancements in neuro-oncology have been impeded by the challenge of delivering therapeutics across the BBB [76]. FUS has emerged as a key technique in this field, enhancing the delivery of both small and large molecular therapeutics to the CNS (Table 1). For instance, MRgFUS has facilitated the transport of molecules such as BCNU [77], cisplatin [78], and doxorubicin [79,80], as well as larger molecules like trastuzumab [81] and adeno-associated viruses [82]. In a pivotal first-in-human study, MRgFUS was demonstrated to be safe for opening the BBB in patients with high-grade gliomas, setting the stage for further clinical trials [1,83].

Subsequent studies, including a multi-center trial, have explored the safety and efficacy of MRgFUS in conjunction with maintenance temozolomide therapy for newly diagnosed glioblastoma multiforme, with results pending publication (NCT03616860, accessed 1 March 2024) [1]. Moreover, the technique's application in enhancing the delivery of radio-labeled therapeutics, such as Indium-111-radiolabeled trastuzumab in patients with Her2-positive breast cancer metastases, has shown promise in reducing tumor volume [84]). Ongoing research, including trials examining the enhanced delivery of pembrolizumab for brain metastases from non-small cell lung cancer, continues to refine the understanding of MRgFUS in clinical practice (NCT05317858). These studies underscore the critical role of pharmacokinetic data and imaging biomarkers in optimizing the therapeutic use of MRgFUS, despite existing gaps in our knowledge [1,83-88] (Table 1).

MRgFUS interventions for Alzheimer's disease

Alzheimer's disease (AD) is a progressive neurodegenerative disorder and the leading cause of

Table 1: FUS-induced BBB opening in neuro-oncology.

Study	Condition & Participants	Device & Treatment Specifications	Key Findings
Mainprize, et al. [83]	Glioblastoma Multiforme (GBM), 5 patients	Utilized ExAblate helmet array with microbubble (MB) injections; a single session conducted before tumor excision. Specifications: 220 kHz frequency, 50% of cavitation threshold. Targeted Area: Tumor margins, measuring 9 × 9 × 6 mm^3	Gadolinium-enhanced MRI verified BBB disruption in peritumoral regions immediately post-sonication. Elevated chemotherapy levels detected in the sonicated areas of 2 patients.
Idbaih, et al. [86]	Recurrent GBM, 19 patients	SonoCloud1 implantable device paired with MB injections followed by intravenous carboplatin. On average, 3 treatment sessions, spaced 4 weeks apart. Specifications: 1 MHz frequency, pressure range 0.41-1.15 MPa (dose escalation)	BBB disruption was successful in 52 out of 65 sonication attempts, with increased effectiveness at higher acoustic pressures. Post-treatment edema occurred in 2 patients, which was responsive to steroid treatment. The study suggested that patients with moderate BBB disruption (grade 2/3) tended to have longer progression-free survival (PFS) and overall survival (OS).
Anastasiadis, et al. [87]	Infiltrative Glioma (WHO grades 2 and 3), 4 patients	ExAblate helmet array with combined with the injection of MB, followed by fluorescein, and ending with surgical excision. Specifications: 230 kHz frequency, power set at 50% of cavitation threshold (mean range: 3-26 W). Targeted Volume: 0.5 cm^3 for patients 1-3, 10 cm^3 for patient 4	No serious adverse events (SAEs) occurred. MRI with gadolinium and intraoperative fluorescence confirmed increased BBB permeability in targeted regions, as validated by histopathological analysis.
Meng, et al. [84]	HER2-positive breast cancer metastasis to the brain, 4 patients	ExAblate helmet array with MB infusion. Specifications: 220 kHz frequency, mean power of 13 W. Entire tumor volumes targeted, with a mean volume of 27 cm^3	Full tumor volumes, including lesions in the posterior fossa, were successfully targeted. No SAEs reported. Trastuzumab delivery to the brain was confirmed via SPECT imaging, and all patients showed a reduction in tumor size.
Sonabend, et al. [88]	Newly resected recurrent GBM, 17 patients	SonoCloud9 implantable device with MB injection. Up to 6 treatments (median 3), followed by intravenous paclitaxel administration with dose escalation. Target: Borders of the resection cavity, mean volume of 12.6 mL	No SAEs reported. BBB was effectively disrupted, with recovery beginning as soon as 1-hour post-treatment. Some patients experienced temporary neurological effects (e.g., paresthesias, aphasia) related to brain regions near the sonication zones. Reversible encephalopathy occurred in two patients at elevated paclitaxel doses.

dementia. Its pathology involves the buildup of toxic amyloid-beta (Aβ) plaques outside neurons, tangles of tau protein inside neurons, neuronal loss, particularly in the circuit of Papez, and dysfunction in the default mode network (DMN) [89-91]. The formation of Aβ plaques is accelerated throughout the brains of AD patients, particularly in areas vulnerable along the DMN, correlating with cognitive decline [92,93]. There is significant interest in using targeted therapies like monoclonal antibodies, including aducanumab and lecanemab, to reduce Aβ plaques in the central nervous system [94]. The FDA approved aducanumab in 2021 based solely on its ability to clear Aβ [95], and lecanemab received approval in 2023 following evidence from a randomized controlled trial showing both Aβ reduction and a modest slowing of cognitive decline [96]. Despite these developments, only a tiny fraction (0.01%) of Aβ antibodies cross the BBB, due to their large molecular size, which the BBB typically filters out, highlighting the need for alternative delivery methods like ultrasound (Table 2) [97,98].

In 2018, the first clinical application of MRgFUS to safely open the BBB in AD patients was reported [59]. This initial study aimed primarily to establish safety, involved opening the BBB in a small region (approximately 9 × 9 × 9 mm) twice, a month apart [59]. T1 gadolinium-enhanced MRI confirmed that the BBB opening was temporary, closing within 24 hours [59]. Subsequent studies expanded on this, demonstrating safe BBB opening over larger volumes and targeting different anatomical sites [99,100]. More recently, MRgFUS was used to open the BBB at major DMN nodes, including the bilateral hippocampi and precuneus, to facilitate drug delivery to these areas [60].

Preclinical studies indicated that FUS could increase aducanumab's penetration into the CNS by 5-8 times [101]. Building on these findings, a recent first-in-human trial utilized MRgFUS to enhance the delivery of aducanumab in three AD patients [102]. The treatment involved six monthly MRgFUS-mediated BBB openings paired with increasing doses of intravenous aducanumab. The amount of brain tissue targeted increased across

Table 2: FUS-induced BBB opening in Alzheimer's disease research.

Study	Condition & Participants	Device & Treatment Specifications	Key Findings
Lipsman, et al. [59]	Alzheimer's Disease (6 patients)	Used ExAblate helmet array with microbubble injections; two sessions spaced one month apart. Parameters: 220 kHz frequency, 4.5 W power (50% of cavitation threshold). Target Area: Right frontal lobe (DLPFC), volume: 1 cm^3	MRI with gadolinium contrast confirmed BBB opening, which closed within 24 hours. No serious adverse events; one patient had temporary neuropsychiatric symptoms, and two patients had transient gradient echo changes, possibly indicating microhemorrhages. No significant change in amyloid levels was observed at the targeted site on PET scans.
Park, et al. [100]	Alzheimer's Disease (6 patients)	Applied ExAblate helmet array with microbubble infusion, two treatments three months apart. Parameters: 220 kHz frequency, 8-40 W power, targeting a cavitation level of 0.4-0.65. Target Area: Bilateral frontal lobes, volume: 21 cm^3	No adverse events were noted. BBB opening was confirmed in 96% of the targeted region by MRI with gadolinium contrast. A 1.6% reduction in amyloid levels was observed in the frontal lobes on PET imaging, with MMSE scores remaining stable and a temporary improvement in neuropsychiatric symptoms.
Epelbaum, et al. [104]	Alzheimer's Disease (10 patients)	Utilized SonoCloud implantable device with microbubble injections, seven sessions every two weeks. Parameters: 1 MHz frequency, 0.9-1.03 MPa pressure, Implant Site: Left supramarginal gyrus, device explanted after 9 months	One patient withdrew due to difficulty activating the device caused by a thick scalp. Another patient experienced a remote hemorrhage leading to acute delirium. Each session lasted 4.5 minutes. A non-significant reduction in amyloid levels was noted around the implant site.
Meng, et al. [60]	Alzheimer's Disease (9 patients)	Employed ExAblate helmet array with microbubble infusion, three sessions two weeks apart. Parameters: 220 kHz frequency, 50% of cavitation threshold power. Target Areas: Default Mode Network (DMN), including bilateral precuneus, anterior cingulate cortex (ACC), and hippocampi (initially unilateral, later bilateral); volume: 9 cm^3	BBB opening was successfully achieved without serious adverse events. Two patients experienced acute confusion, with one case lasting a week, leading to that patient being excluded from further procedures. Immediate gradient echo changes were observed in two patients, which resolved the next day. A small but significant reduction in beta amyloid was detected in the sonicated right parahippocampal/inferior temporal region via PET imaging.
Rezai, et al. [105]	Alzheimer's Disease (10 patients)	Deployed ExAblate helmet array with microbubble injections/infusions, three sessions two weeks apart. Parameters: 220 kHz frequency, initial target: Unilateral hippocampus/entorhinal cortex (EC), later expanded to include frontal and parietal regions (up to 30 cm^3)	No serious adverse events were reported. One patient developed hippocampal edema, which resolved within 72 hours. MRI-Gad showed BBB opening in 82% of the targeted brain volume, with closure within 24-48 hours. Cognitive assessments (ADAS-Cog/MMSE) showed stable cognition at 6 months and a mild decline at 12 months, consistent with expected progression.
Rezai, et al. [102]	Alzheimer's Disease (3 patients)	Used ExAblate helmet array with microbubble infusions, six monthly treatments paired with aducanumab infusion 2 hours prior. Parameters: 220 kHz frequency, Target Areas: Patient 1: right frontal lobe (10 mL), Patient 2: left frontal/ parietal lobe (20 mL), Patient 3: left frontal/ parietal/temporal lobes & hippocampus (40 mL)	Patient 3 showed cognitive decline after 30 days, without affecting daily activities. A significant reduction in amyloid levels was observed in the treated regions compared to baseline and untreated contralateral areas on PET imaging.

ACC: Anterior Cingulate Cortex; ADAS-Cog: Alzheimer Disease Assessment Scale-Cognitive Subscale; DLPFC: Dorsolateral Prefrontal Cortex; EC: Entorhinal Cortex; MMSE: Mini-Mental State Examination

patients, from 10 mL in the non-dominant frontal lobe of the first patient to 40 mL in the dominant frontal, temporal, and hippocampal regions of the third patient. Aβ reduction was observed in the treated areas using fluorine-18 florbetaben positron emission tomography (PET) scans, with untreated homologous brain regions serving as controls [102]. However, the third patient experienced cognitive decline by the 30-day follow-up, raising challenges in distinguishing between natural disease progression and potential adverse effects of the treatment. Additionally, there remains uncertainty about whether reducing Aβ levels directly correlates with cognitive improvement [103] (Table 2).

Therapeutic innovations for Parkinson's disease

using MRgFUS

Parkinson's disease (PD) is the most prevalent neurodegenerative movement disorder, affecting 1% of individuals over the age of 60 [106]. The hallmark motor symptoms of PD are due to the loss of dopaminergic neurons in the substantia nigra pars compacta, accompanied by Lewy body pathology, resulting in reduced dopamine levels in the striatum [107]. The exact causes of PD are still being explored, but they likely involve a combination of lifestyle factors, environmental exposures, and genetic predispositions [108]. While aging is the primary risk factor, other contributors include exposure to toxins like rotenone and paraquat [109] and genetic mutations such as those in the GBA1 [110,111] and LRRK2 genes [112]. As in Alzheimer's disease and neuro-oncology, BBB has been a significant challenge for PD therapies, sparking interest in using FUS to enhance the delivery of treatments targeting alpha-synuclein or neurotrophic factors to the basal ganglia [113].

In preclinical models, studies have shown that the BBB can be safely opened in the putamen [114]. When combined with alpha-synuclein silencing viral vectors or neurotrophic factors, this approach can reduce nigrostriatal neuron loss in MPTP or transgenic mouse models [115,116]. A recent study highlighted the use of MRgFUS to open the BBB, combined with systemic administration of an AAV vector, inducing novel protein expression in the putamen and substantia nigra, which may offer a new strategy for protein modulation in PD patients [61]. However, challenges include the high cost of systemic AAV delivery at effective doses for human transduction and potential risks from systemic exposure, even with improved BBB permeability. Advances in neuron-selective AAV serotypes with minimal systemic uptake may provide a solution for integrating gene therapy with MRgFUS [117].

In clinical settings, MRgFUS-mediated BBB opening in the putamen has shown good tolerance in PD patients, including in bilateral and repeated treatments [91]. The putamen is sensitive to physical damage [118], yet MRgFUS treatments have not shown exacerbation of dopaminergic denervation in imaging studies, although data remain limited and further research is needed to define safety thresholds [119]. The first clinical use of MRgFUS-mediated BBB opening paired with drug delivery was recently reported in PD patients with GBA1 mutations, which are linked to Gaucher's disease [120]. GBA1 encodes the enzyme glucocerebrosidase (GCase), and preclinical studies suggest that a deficiency or reduced activity of GCase leads to alpha-synuclein accumulation, which may contribute to dopaminergic neuron loss [121,122]. Intravenous recombinant GCase is a promising therapy for PD in the context of GBA1 mutations, though its penetration of the BBB is limited [123].

A study was conducted to evaluate the safety of combining MRgFUS-mediated BBB opening with intravenous GCase administration in patients with GBA1-related PD [124]. Four patients underwent a total of three MRgFUS procedures, each followed by an increasing dose of GCase, spaced two weeks apart. Gadolinium-enhanced MRI confirmed successful unilateral BBB opening in the putamen without severe adverse effects [120]. Two patients reported transient increases in dyskinesia, possibly due to increased levodopa exposure from BBB permeabilization [120]. Positron emission tomography (PET) scans showed reduced metabolism in the putamen one-month post-treatment, correlating with treatment efficacy seen in other studies [125]. This phase 1 trial lays the groundwork for targeted delivery of GCase and other therapeutic molecules, such as neurotrophins or monoclonal antibodies, for movement disorders. Future research will focus on understanding the safety of MRgFUS in PD patients and the pharmacodynamics of GCase when delivered via ultrasound.

Advanced Neurological Therapies with MRgFUS

MRgFUS-enhanced immunotherapy

Research on the use of immunotherapy combined with MRgFUS for treating brain tumors has primarily focused on delivering HER2-targeting antibodies for breast cancer metastases. In a mouse model, FUS successfully delivered trastuzumab, although the dosage was limited due to red blood cell extravasation [81]. Without MRgFUS, trastuzumab levels in brain tissue were undetectable except in one case. In a rat model of HER2-positive human breast cancer brain metastases, Park, et al. demonstrated that MRgFUS-enhanced delivery of trastuzumab extended the median survival time compared to no treatment (83 days *vs*. 63 days) and trastuzumab alone (83 days vs. 71 days, not statistically significant), with a significant reduction in tumor volume at week 7 [126]. Notably, this effect was observed in a subset of the experimental group, as 6 of the 10 treated mice did not respond. Rats treated with MRgFUS and HER2-specific NK-92 cells administered peripherally showed increased mean survival times [127]. Similar to Park, et al.'s findings, approximately half of the treated animals were non-responders, exhibiting survival curves similar to untreated animals. The study did not observe histological evidence of red blood cell extravasation, possibly because there was a delay of a week or more between the last MRgFUS treatment and euthanasia.

In a rat glioma model, FUS increased the concentration of intraperitoneal IL-12 in the brain nearly 2.9-fold compared to no FUS [128]. The combination of IL-12 and FUS significantly increased the presence of T-lymphocytes within the tumors compared to sham

treatment (CD3+ CD4+: more than 4-fold increase; CD3+ CD8+: 5-fold increase; CD4+ CD25+: 2-fold increase; cytotoxic-to-regulatory T-cell ratio increase: 2.5-fold). These effects were not observed in healthy rats or systemically in tumor-bearing rats. The median survival time was also longer compared to no treatment (30 days *vs*. 21 days) and IL-12 alone (30 days *vs*. 26 days). The promising results in animal models suggest that immunotherapies could potentially be integrated into MRgFUS treatment protocols, pending further research to optimize targeting strategies [128].

Gene therapy augmentation with MRgFUS

The use FUS to deliver DNA-loaded microbubbles represents a novel approach in the field. In a rat glioma model, folate-conjugated cationic microbubbles (cMBs) containing DNA were used in conjunction with ultrasound targeting, resulting in successful transfection of tumor cells. This treatment increased reporter gene expression in tumor tissue by 4.7 times compared to direct injection and by 1.5 times compared to cMBs without folate conjugation, with expression localized exclusively within the tumor [129]. Another study in a rat glioma model used DNA-loaded cMBs conjugated with VEGFR2-targeted monoclonal antibodies. This approach resulted in reporter gene expression that was 3.7 times higher with targeted cMBs and 2.3 times higher with non-targeted cMBs compared to direct DNA injection [130]. Additionally, the study explored the use of cMBs with the suicide gene pHSV-TK, which converts ganciclovir into a compound that halts DNA replication, leading to tumor cell death [131]. The combination of cMBs and FUS significantly reduced tumor volume at day 25 compared to direct injection (9.7 ± 5.2 mm^3 *vs*. 40.1 ± 4.3 mm^3) and non-targeted cMBs (9.7 ± 5.2 mm^3 *vs*. 21.8 ± 4.7 mm^3). Both targeted and non-targeted cMBs led to a significant reduction in tumor volume and an increase in median survival time compared to untreated controls [131].

Gene therapy, among brain tumor treatments using FUS, remains the least developed. As this technology progresses towards clinical trials, incorporating MR guidance will be crucial for imaging through the human skull.

Challenges and Considerations of MRgFUS

While preclinical studies in animal models have shown promise, comprehensive testing in humans is necessary. A Phase 1 clinical trial is essential to assess toxicity and establish safe parameters for the strength of MRgFUS, as well as to optimize the selection, dosage, and timing of systemic chemotherapeutic agents. The human skull is thicker than that of rodents, and the greater distances within the human cranium can reduce ultrasound intensity, necessitating higher power levels. The depth of tumors may also restrict the types of lesions that can be effectively treated [30]. Moreover, severe or symptomatic peritumoral edema might worsen with further disruption of the BTB. Using stereotactic frames poses challenges for patients needing multiple FUS treatments, but frameless systems are in development [31]. The risk of hemorrhage has been observed in animal models, but it remains unclear how this will manifest in human patients [67,81].

Conclusion

MRgFUS offers a significant advancement in non-invasive, targeted drug delivery for brain tumors. By combining MRgFUS with other technologies such as nanoparticles, the precision and effectiveness of treatments can be significantly enhanced. Preclinical studies have shown that MRgFUS improves the delivery and efficacy of chemotherapy, immunotherapy, and gene therapy, leading to better treatment outcomes, reduced tumor growth, and extended survival times.

Looking ahead, there is growing interest in applying MRgFUS-mediated BBB opening to a broader range of neurological conditions, including Alzheimer's disease, Parkinson's disease, and neuro-oncological disorders. As clinical trials expand and involve larger cohorts, a more comprehensive understanding of the biological effects of drugs delivered via MRgFUS will emerge, allowing for more precise dosing and optimized treatment schedules. Randomized controlled trials will likely provide more detailed data on the efficacy of this method across different indications.

Technological advancements in MRgFUS devices, such as the development of frameless systems and minimally invasive procedures, are anticipated to further enhance the method's accessibility and patient comfort. These innovations will be essential for integrating MRgFUS into standard therapeutic protocols, potentially transforming the treatment landscape for patients with complex neurological conditions.

References

1. Meng Y, Kalia LV, Kalia SK, Hamani C, Huang Y, et al. (2024) Current progress in magnetic resonance-guided focused ultrasound to facilitate drug delivery across the blood-brain barrier. Pharmaceutics 16: 719.
2. Pardridge WM (2005) The blood-brain barrier: Bottleneck in brain drug development. NeuroRx 2: 3-14.
3. Daneman R, Prat A (2015) The blood-brain barrier. Cold Spring Harb Perspect Biol 7: a020412.
4. Akhtar A, Andleeb A, Waris TS, Bazzar M, Moradi AR, et al. (2021) Neurodegenerative diseases and effective drug delivery: A review of challenges and novel therapeutics. J Control Release 330: 1152-1167.
5. Stamp ME, Halwes M, Nisbet D, Collins DJ (2023) Breaking barriers: Exploring mechanisms behind opening the blood-brain barrier. Fluids Barriers CNS 20: 87.
6. Wang D, Wang C, Wang L, Chena Y (2019) A comprehensive review in improving delivery of small-molecule chemotherapeutic agents overcoming the blood-brain/brain tumor barriers for glioblastoma treatment. Drug

Deliv 26: 551-565.

7. Meng Y, People CB, Lea-Banks H, Abrahao A, Davidson B, et al. (2019) Safety and efficacy of focused ultrasound induced blood-brain barrier opening, an integrative review of animal and human studies. J Control Release 309: 25-36.

8. Meng Y, Huang Y, Solomon B, Hynynen K, Scantlebury N, et al. (2017) MRI-guided focused ultrasound thalamotomy for patients with medically-refractory essential tremor. J Vis Exp 56365.

9. Davidson B, Hamani C, Rabin JS, Goubran M, Meng Y, et al. (2020) Magnetic resonance-guided focused ultrasound capsulotomy for refractory obsessive compulsive disorder and major depressive disorder: Clinical and imaging results from two phase I trials. Mol Psychiatry 25: 1946-1957.

10. Hynynen K, McDannold N, Vykhodtseva N, Jolesz FA (2001) Noninvasive MR imaging-guided focal opening of the blood-brain barrier in rabbits. Radiology 220: 640-646.

11. Meng Y, Hynynen K, Lipsman N (2021) Applications of focused ultrasound in the brain: From thermoablation to drug delivery. Nat Rev Neurol 17: 7-22.

12. Arsiwala T, Sprowls SA, Blethen KE, Adkins CE, Saralkar PA, et al. (2021) Ultrasound-mediated disruption of the blood tumor barrier for improved therapeutic delivery. Neoplasia 23: 676-691.

13. Carpentier A, Stupp R, Sonabend AM, Dufour H, Chinot O, et al. (2024) Repeated blood-brain barrier opening with a nine-emitter implantable ultrasound device in combination with carboplatin in recurrent glioblastoma: A phase I/II clinical trial. Nat Commun 15: 1650.

14. Lamsam L, Johnson E, Connolly ID, Wintermark M, Gephart MH (2018) A review of potential applications of MR-guided focused ultrasound for targeting brain tumor therapy. Neurosurg Focus 44: E10.

15. Liu Y, Lu W (2012) Recent advances in brain tumor-targeted nano-drug delivery systems. Expert Opin Drug Deliv 9: 671-686.

16. Downs ME, Buch A, Sierra C, Karakatsani ME, Chen S, et al. (2015) Long-term safety of repeated blood-brain barrier opening via focused ultrasound with microbubbles in non-human primates performing a cognitive task. PLoS One 10: e0125911.

17. Coluccia D, Fandino J, Schwyzer L, O'Gorman R, Remonda L, et al. (2014) First noninvasive thermal ablation of a brain tumor with MR-guided focusedultrasound. J Ther Ultrasound 2: 17.

18. De Bock M, Wang N, Decrock E, Bol M, Gadicherla AK, et al. (2013) Endothelial calcium dynamics, connexin channels and blood-brain barrier function. Prog Neurobiol 108: 1-20.

19. Debinski W, Tatter SB (2009) Convection-enhanced delivery for the treatment of brain tumors. Expert Rev Neurother 9: 1519-1527.

20. Fry W (1950) Physical factors involved in ultrasonically induced changes in living systems: Identification of non□ temperature effects. JASA 22: 867-876.

21. Hill CR, Bamber JC, Ter Haar GR (2004) Physical principles of medical ultrasonics. John Wiley & Sons.

22. Bailey MR, Khokhlova VA, Sapozhnikov OA, Kargl SG, Crum LA (2003) Physical mechanisms of the therapeutic effect of ultrasound (a review). Acoustical Physics 49: 369-388.

23. Gourevich D, Dogadkin O, Volovick A, Wang L, Gnaim J, et al. (2013) Ultrasound-mediated targeted drug delivery with a novel cyclodextrin-based drug carrier by mechanical and thermal mechanisms. J Control Release 170: 316-324.

24. Tempany CMC, Stewart EA, McDannold N, Quade BJ, Jolesz FA, et al. (2003) MR imaging-guided focused ultrasound surgery of uterine leiomyomas: A feasibility study. Radiology 226: 897-905.

25. Kim YS, Keserci B, Partanen A, Rhim H, Lim HK, et al. (2012) Volumetric MR-HIFU ablation of uterine fibroids: Role of treatment cell size in the improvement of energy efficiency. Eur J Radiol 81: 3652-3659.

26. Hynynen K, Pomeroy O, Smith DN, Huber PE, McDannold NJ, et al. (2001) MR imaging-guided focused ultrasound surgery of fibroadenomas in the breast: A feasibility study. Radiology 219: 176-185.

27. Furusawa H, Namba K, Nakahara H, Tanaka C, Yasuda Y, et al. (2007) The evolving non-surgical ablation of breast cancer: MR guided focused ultrasound (MRgFUS). Breast Cancer 14: 55-58.

28. Chopra R, Colquhoun A, Burtnyk M, N'djin WA, Kobelevskiy I, et al. (2012) MR imaging-controlled transurethral ultrasound therapy for conformal treatment of prostate tissue: Initial feasibility in humans. Radiology 265: 303-313.

29. Liberman B, Gianfelice D, Inbar Y, Beck A, Rabin T, et al. (2009) Pain palliation in patients with bone metastases using MR-guided focused ultrasound surgery: A multicenter study. Ann Surg Oncol 16: 140-146.

30. McDannold N, Clement G, Black P, Jolesz F, Hynynen K (2010) Transcranial magnetic resonance imaging-guided focused ultrasound surgery of brain tumors: Initial findings in 3 patients. Neurosurgery 66: 323-332.

31. Martin E, Jeanmonod D, Morel A, Zadicario E, Werner B (2009) High□intensity focused ultrasound for noninvasive functional neurosurgery. Ann Neurol 66: 858-861.

32. Jeanmonod D, Werner B, Morel A, Michels L, Zadicario E, et al. (2012) Transcranial magnetic resonance imaging-guided focused ultrasound: Noninvasive central lateral thalamotomy for chronic neuropathic pain. Neurosurg Focus 32: E1.

33. Tyler WJ, Tufail Y, Pati S (2010) Pain: Noninvasive functional neurosurgery using ultrasound. Nat Rev Neurol 6: 13-14.

34. Haen SP, Pereira PL, Salih HR, Rammensee HG, Gouttefangeas C (2011) More than just tumor destruction: Immunomodulation by thermal ablation of cancer. J Immunol Res 2011: 160250.

35. Marty B, Larrat B, Landeghem MV, Robic C, Robert P, et al. (2012) Dynamic study of blood-brain barrier closure after its disruption using ultrasound: A quantitative analysis. J Cereb Blood Flow Metab 32: 1948-1958.

36. Jung NY, Chang JW (2018) Magnetic resonance-guided focused ultrasound in neurosurgery: Taking lessons from the past to inform the future. J Korean Med Sci 33: e279.

37. Harary M, Segar DJ, Huang KT, Tafel IJ, Valdes PA, et al. (2018) Focused ultrasound in neurosurgery: A historical perspective. Neurosurg Focus 44: E2.

38. Ishimaru A (1978) Wave propagation and scattering in random media. Academic press New York: 2.

39. Laugier P, Haïat G (2010) Introduction to the physics of ultrasound. Bone Quantitative Ultrasound 29-45.

40. Christian E, Yu C, Apuzzo MLJ (2014) Focused ultrasound: Relevant history and prospects for the addition of mechanical energy to the neurosurgical armamentarium. World Neurosurg 82: 354-365.

41. Jolesz FA (2009) MRI-guided focused ultrasound surgery. Annu Rev Med 60: 417-430.

42. Tempany CM, McDannold NJ, Hynynen K, Jolesz FA (2011) Focused ultrasound surgery in oncology: Overview and principles. Radiology 259: 39-56.

43. Jagannathan J, Sanghvi NT, Crum LA, Yen CP, Medel R, et al. (2009) High-intensity focused ultrasound surgery of the brain: Part 1--A historical perspective with modern applications. Neurosurgery 64: 201-211.

44. Gruetzmacher J (1935) Piezoelektrischer kristall mit ultraschallkonvergenz. Zeitschrift für Physik 96: 342-349.

45. Hynynen K, Vykhodtseva NI, Chung AH, Sorrentino V, Colucci V, et al. (1997) Thermal effects of focused ultrasound on the brain: Determination with MR imaging. Radiology 204: 247-253.

46. Hynynen K, Jolesz FA (1998) Demonstration of potential noninvasive ultrasound brain therapy through an intact skull. Ultrasound Med Biol 24: 275-283.

47. Hynynen K, McDannold N, Sheikov NA, Jolesz FA, Vykhodtseva N (2005) Local and reversible blood-brain barrier disruption by noninvasive focused ultrasound at frequencies suitable for trans-skull sonications. Neuroimage 24: 12-20.

48. Sheikov N, McDannold N, Vykhodtseva N, Jolesz F, Hynynen K (2004) Cellular mechanisms of the blood-brain barrier opening induced by ultrasound in presence of microbubbles. Ultrasound Med Biol 30: 979-989.

49. Abrahao A, Meng Y, Llinas M, Huang Y, Hamani C, et al. (2019) First-in-human trial of blood-brain barrier opening in amyotrophic lateral sclerosis using MR-guided focused ultrasound. Nat Commun 10: 4373.

50. Dijkmans P, Juffermans LJM, Musters RJP, van Wamel A, ten Cate FJ, et al. (2004) Microbubbles and ultrasound: From diagnosis to therapy. Eur J Echocardiogr 5: 245-246.

51. Chopra R, Vykhodtseva N, Hynynen K (2010) Influence of exposure time and pressure amplitude on blood-brain-barrier opening using transcranial ultrasound exposures. ACS Chem Neurosci 1: 391-398.

52. O'Reilly MA, Hough O, Hynynen K (2017) Blood□brain barrier closure time after controlled ultrasound□induced opening is independent of opening volume. J Ultrasound Med 36: 475-483.

53. Aryal M, Fischer K, Gentile C, Gitto S, Zhang Y, et al. (2017) Effects on P-glycoprotein expression after blood-brain barrier disruption using focused ultrasound and microbubbles. PLoS One 12: e0166061.

54. O'Reilly MA, Waspe AC, Chopra R, Hynynen K (2012) MRI-guided disruption of the blood-brain barrier using transcranial focused ultrasound in a rat model. J Vis Exp 61: e3555.

55. Grasso G, Torregrossa F, Noto M, Bruno E, Feraco P, et al. (2023) MR-guided focused ultrasound-induced blood-brain barrier opening for brain metastasis: A review. Neurosurg Focus 55: E11.

56. Wu SK, Chu PC, Chai WY, Kang ST, Tsai CH, et al. (2017) Characterization of different microbubbles in assisting focused ultrasound-induced blood-brain barrier opening. Sci Rep 7: 46689.

57. McDannold N, Arvanitis CD, Vykhodtseva N, Livingstone MS (2012) Temporary disruption of the blood-brain barrier by use of ultrasound and microbubbles: Safety and efficacy evaluation in rhesus macaques. Cancer Res 72: 3652-3663.

58. McDannold N, Vykhodtseva N, Hynynen K (2008) Blood-brain barrier disruption induced by focused ultrasound and circulating preformed microbubbles appears to be characterized by the mechanical index. Ultrasound Med Biol 34: 834-840.

59. Lipsman N, Meng Y, Bethune AJ, Huang Y, Lam B, et al. (2018) Blood-brain barrier opening in Alzheimer's disease using MR-guided focused ultrasound. Nat Commun 9: 2336.

60. Meng Y, Goubran M, Rabin JS, McSweeney M, Ottoy J, et al. (2023) Blood-brain barrier opening of the default mode network in Alzheimer's disease with magnetic resonance-guided focused ultrasound. Brain 146: 865-872.

61. Blesa J, Pineda-Pardo JA, Inoue KI, Gasca-Salas C, Balzano T, et al. (2023) BBB opening with focused ultrasound in nonhuman primates and Parkinson's disease patients: Targeted AAV vector delivery and PET imaging. Sci Adv 9: eadf4888.

62. Lea-Banks H, Hynynen K (2021) Sub-millimetre precision of drug delivery in the brain from ultrasound-triggered nanodroplets. J Control Release 338: 731-741.

63. Gouveia FV, Lea□Banks H, Aubert I, Lipsman N, Hynynen K, et al. (2023) Anesthetic□loaded nanodroplets with focused ultrasound reduces agitation in Alzheimer's mice. Ann Clin Transl Neurol 10: 507-519.

64. Chen YX, Feng PJ, Zhong G, Liu JH, Jiang B, et al. (2024) Piezoelectric nanogenerators enabled neuromodulation rescued dopaminergic neuron loss in Parkinson's disease. Nano Energy 121: 109187.

65. Mikhail AS, Partanen A, Yarmolenko P, Venkatesan AM, Wood BJ (2015) Magnetic resonance-guided drug delivery. Magn Reson Imaging Clin N Am 23: 643-655.

66. Staruch RM, Hynynen K, Chopra R (2015) Hyperthermia-mediated doxorubicin release from thermosensitive liposomes using MR-HIFU: Therapeutic effect in rabbit Vx2 tumours. Int J Hyperthermia 31: 118-133.

67. Park J, Aryal M, Vykhodtseva N, Zhang YZ, McDannold N (2017) Evaluation of permeability, doxorubicin delivery, and drug retention in a rat brain tumor model after ultrasound-induced blood-tumor barrier disruption. J Control Release 250: 77-85.

68. Liu HL, Hua MY, Chen PY, Chu PC, Pan CH, et al. (2010) Blood-brain barrier disruption with focused ultrasound enhances delivery of chemotherapeutic drugs for glioblastoma treatment. Radiology 255: 415-425.

69. Wei KC, Chu PC, Jack Wang HY, Huang CY, Chen PY, et al. (2013) Focused ultrasound-induced blood-brain barrier opening to enhance temozolomide delivery for glioblastoma treatment: A preclinical study. PLoS One 8: e58995.

70. Iwamoto T (2013) Clinical application of drug delivery systems in cancer chemotherapy: Review of the efficacy and side effects of approved drugs. Biol Pharm Bull 36: 715-718.

71. Chertok B, Moffat BA, David AE, Faquan Yu, Bergemann C, et al. (2008) Iron oxide nanoparticles as a drug delivery vehicle for MRI monitored magnetic targeting of brain tumors. Biomaterials 29: 487-496.

72. Veiseh O, Gunn JW, Zhang M (2010) Design and fabrication

of magnetic nanoparticles for targeted drug delivery and imaging. Adv Drug Deliv Rev 62: 284-304.

73. Liu HL, Hua MY, Yang HW, Huang CY, Chu PC, et al. (2010) Magnetic resonance monitoring of focused ultrasound/magnetic nanoparticle targeting delivery of therapeutic agents to the brain. Proc Natl Acad Sci U S A 107: 15205-15210.

74. Chen PY, Liu HL, Hua MY, Yang HW, Huang CY, et al. (2010) Novel magnetic/ultrasound focusing system enhances nanoparticle drug delivery for glioma treatment. Neuro Oncol 12: 1050-1060.

75. Fan CH, Ting CY, Lin HJ, Wang CH, Liu HL, et al. (2013) SPIO-conjugated, doxorubicin-loaded microbubbles for concurrent MRI and focused-ultrasound enhanced brain-tumor drug delivery. Biomaterials 34: 3706-3715.

76. Aldape K, Brindle KM, Chesler L, Chopra R, Gajjar A, et al. (2019) Challenges to curing primary brain tumours. Nat Rev Clin Oncol 16: 509-520.

77. Fan CH, Ting CY, Chang YC, Wei KC, Liu HL, et al. (2015) Drug-loaded bubbles with matched focused ultrasound excitation for concurrent blood-brain barrier opening and brain-tumor drug delivery. Acta Biomater 15: 89-101.

78. Alli S, Figueiredo CA, Golbourn B, Sabha N, Wu MY, et al. (2018) Brainstem blood brain barrier disruption using focused ultrasound: A demonstration of feasibility and enhanced doxorubicin delivery. J Control Release 281: 29-41.

79. Martinez PJ, Green AL, Borden MA (2024) Targeting diffuse midline gliomas: The promise of focused ultrasound-mediated blood-brain barrier opening. J Control Release 365: 412-421.

80. Lin YL, Wu MT, Yang FY (2018) Pharmacokinetics of doxorubicin in glioblastoma multiforme following ultrasound-Induced blood-brain barrier disruption as determined by microdialysis. J Pharm Biomed Anal 149: 482-487.

81. Kinoshita M, McDannold N, Jolesz FA, Hynynen K (2006) Noninvasive localized delivery of Herceptin to the mouse brain by MRI-guided focused ultrasound-induced blood-brain barrier disruption. Proc Natl Acad Sci U S A 103: 11719-11723.

82. Timbie KF, Mead BP, Price RJ (2015) Drug and gene delivery across the blood-brain barrier with focused ultrasound. J Control Release 219: 61-75.

83. Mainprize T, Lipsman N, Huang Y, Meng Y, Bethune A, et al. (2019) Blood-brain barrier opening in primary brain tumors with non-invasive MR-guided focused ultrasound: A clinical safety and feasibility study. Sci Rep 9: 321.

84. Meng Y, Reilly RM, Pezo RC, Trudeau M, Sahgal A, et al. (2021) MR-guided focused ultrasound enhances delivery of trastuzumab to Her2-positive brain metastases. Sci Transl Med 13: eabj4011.

85. Cho NS, Wong WK, Nghiemphu PL, Cloughesy TF, Ellingson BM (2023) The Future Glioblastoma Clinical Trials Landscape: Early Phase 0, Window of Opportunity, and Adaptive Phase I-III Studies. Curr Oncol Reports 25: 1047-1055.

86. Idbaih A, Canney M, Belin L, Desseaux C, Vignot A, et al. (2019) Safety and feasibility of repeated and transient blood-brain barrier disruption by pulsed ultrasound in patients with recurrent glioblastoma. Clin Cancer Res 25: 3793-3801.

87. Anastasiadis P, Gandhi D, Guo Y, Ahmed AK, Bentzen SM, et al. (2021) Localized blood-brain barrier opening in infiltrating gliomas with MRI-guided acoustic emissions-controlled focused ultrasound. Proc Natl Acad Sci U S A 118: e2103280118.

88. Sonabend AM, Gould A, Amidei C, Ward R, Schmidt KA, et al. (2023) Repeated blood-brain barrier opening with an implantable ultrasound device for delivery of albumin-bound paclitaxel in patients with recurrent glioblastoma: A phase 1 trial. Lancet Oncol 24: 509-522.

89. Busche MA, Hyman BT (2020) Synergy between amyloid-β and tau in Alzheimer's disease. Nat Neurosci 23: 1183-1193.

90. Selkoe DJ, Hardy J (2016) The amyloid hypothesis of Alzheimer's disease at 25 years. EMBO Mol Med 8: 595-608.

91. Contreras JA, Avena-Koenigsberger A, Risacher SL, West JD, Tallman E, et al. (2019) Resting state network modularity along the prodromal late onset Alzheimer's disease continuum. Neuroimage Clin 22: 101687.

92. Palmqvist S, Schöll M, Strandberg O, Mattsson N, Stomrud E, et al. (2017) Earliest accumulation of β-amyloid occurs within the default-mode network and concurrently affects brain connectivity. Nat Commun 8: 1214.

93. Pascoal TA, Mathotaarachchi S, Kang MS, Mohaddes S, Shin M, et al. (2019) Aβ-induced vulnerability propagates via the brain's default mode network. Nat Commun 10: 2353.

94. Kumaran KR, Yunusa S, Perimal E, Wahab H, Müller CP, et al. (2023) Insights into the pathophysiology of Alzheimer's disease and potential therapeutic targets: A current perspective. J Alzheimers Dis 91: 507-530.

95. Mullard A (2021) News in focus. Nature 594: 309.

96. Van Dyck CH, Swanson CJ, Aisen P, Bateman RJ, Chen C, et al. (2023) Lecanemab in early Alzheimer's disease. N Engl J Med 388: 9-21.

97. Banks WA, Terrell B, Farr SA, Robinson SM, Nonaka N, et al. (2002) Passage of amyloid β protein antibody across the blood-brain barrier in a mouse model of Alzheimer's disease. Peptides 23: 2223-2226.

98. Blennow K, Zetterberg H, Rinne JO, Salloway S, Wei J, et al. (2012) Effect of immunotherapy with bapineuzumab on cerebrospinal fluid biomarker levels in patients with mild to moderate Alzheimer disease. Arch Neurol 69: 1002-1010.

99. Rezai AR, Ranjan M, D'Haese PF, Haut MW, Carpenter J, et al. (2020) Noninvasive hippocampal blood-brain barrier opening in Alzheimer's disease with focused ultrasound. Proc Natl Acad Sci U S A 117: 9180-9182.

100. Park SH, Baik K, Jeon S, Chang WS, Ye BK, et al. (2021) Extensive frontal focused ultrasound mediated blood-brain barrier opening for the treatment of Alzheimer's disease: A proof-of-concept study. Transl Neurodegener 10: 44.

101. Kong C, Yang EJ, Shin J, Park J, Kim SH, et al. (2022) Enhanced delivery of a low dose of aducanumab via FUS in 5× FAD mice, an AD model. Transl Neurodegener 11: 57.

102. Rezai AR, D'Haese PF, Finomore V, Carpenter J, Ranjan M, et al. (2024) Ultrasound blood-brain barrier opening and aducanumab in Alzheimer's disease. N Engl J Med 390: 55-62.

103. Gulisano W, Maugeri D, Baltrons MA, Fà M, Amato A, et al. (2018) Role of amyloid-β and tau proteins in Alzheimer's

disease: Confuting the amyloid cascade. J Alzheimers Dis 64: S611-S631.

104. Epelbaum S, Burgos N, Canney M, Matthews D, Houot M, et al. (2022) Pilot study of repeated blood-brain barrier disruption in patients with mild Alzheimer's disease with an implantable ultrasound device. Alzheimers Res Ther 14: 40.

105. Rezai AR, Ranjan M, Haut MW, Carpenter J, D'Haese PF, et al. (2022) Focused ultrasound-mediated blood-brain barrier opening in Alzheimer's disease: Long-term safety, imaging, and cognitive outcomes. J Neurosurg 139: 275-283.

106. de Lau LML, Breteler MMB (2006) Epidemiology of Parkinson's disease. Lancet Neurol 5: 525-535.

107. Dauer W, Przedborski S (2003) Parkinson's disease: Mechanisms and models. Neuron 39: 889-909.

108. Kalia LV, Lang AE (2015) Parkinson's disease. Lancet 386: 896-912.

109. Tanner CM, Kamel F, Ross GW, Hoppin JA, Goldman SM, et al. (2011) Rotenone, paraquat, and Parkinson's disease. Environ Health Perspect 119: 866-872.

110. Sidransky E, Lopez G (2012) The link between the GBA gene and parkinsonism. Lancet Neurol 11: 986-998.

111. Cilia R, Tunesi S, Marotta G, Cereda E, Siri C, et al. (2016) Survival and dementia in GBA□associated Parkinson's disease: The mutation matters. Ann Neurol 80: 662-673.

112. Zimprich A, Biskup S, Leitner P, Lichtner P, Farrer M, et al. (2004) Mutations in LRRK2 cause autosomal-dominant parkinsonism with pleomorphic pathology. Neuron 44: 601-607.

113. Meng Y, Voisin MR, Suppiah S, Kalia SK, Kalia LV, et al. (2018) Is there a role for MR-guided focused ultrasound in Parkinson's disease? Mov Disord 33: 575-579.

114. Karakatsani ME, Blesa J, Konofagou EE (2019) Blood-brain barrier opening with focused ultrasound in experimental models of Parkinson's disease. Mov Disord 34: 1252-1261.

115. Karakatsani ME, Wang S, Samiotaki G, Kugelman T, Olumolade OO, et al. (2019) Amelioration of the nigrostriatal pathway facilitated by ultrasound-mediated neurotrophic delivery in early Parkinson's disease. J Control Release 303: 289-301.

116. Xhima K, Nabbouh F, Hynynen K, Aubert I, Tandon A, et al. (2018) Noninvasive delivery of an α□synuclein gene silencing vector with magnetic resonance-guided focused ultrasound. Mov Disord 33: 1567-1579.

117. Challis RC, Kumar SR, Chen X, Goertsen D, Coughlin GM, et al. (2022) Adeno-associated virus toolkit to target diverse brain cells. Annu Rev Neurosci 45: 447-469.

118. Bhatia KP, Marsden CD (1994) The behavioural and motor consequences of focal lesions of the basal ganglia in man. Brain 117: 859-876.

119. Pineda□Pardo JA, Gasca-Salas C, Fernández-Rodríguez B, Rodríguez-Rojas R, Del Álamo M, et al. (2022) Striatal blood-brain barrier opening in Parkinson's disease dementia: A pilot exploratory study. Mov Disord 37: 2057-2065.

120. Meng Y, Pople CB, Huang Y, Jones RM, Ottoy J, et al. (2022) Putaminal Recombinant Glucocerebrosidase Delivery with Magnetic Resonance–Guided Focused Ultrasound in Parkinson's Disease: A Phase I Study. Mov Disord 37: 2134-2139.

121. Cerri S, Ghezzi C, Sampieri M, Siani F, Avenali M, et al. (2018) The exosomal/total α-synuclein ratio in plasma is associated with glucocerebrosidase activity and correlates with measures of disease severity in PD patients. Front Cell Neurosci 12: 125.

122. Sardi SP, Clarke J, Kinnecom C, Tamsett TJ, Li L, et al. (2011) CNS expression of glucocerebrosidase corrects α-synuclein pathology and memory in a mouse model of gaucher-related synucleinopathy. Proc Natl Acad Sci U S A 108: 12101-12106.

123. Gegg ME, Menozzi E, Schapira AH (2022) Glucocerebrosidase-associated Parkinson disease: Pathogenic mechanisms and potential drug treatments. Neurobiol Dis 166: 105663.

124. Huang Y, Meng Y, Pople CB, Bethune A, Jones RM, et al. (2022) Cavitation feedback control of focused ultrasound blood-brain barrier opening for drug delivery in patients with Parkinson's disease. Pharmaceutics 14: 2607.

125. Hirano S, Eckert T, Flanagan T, Eidelberg D (2009) Metabolic networks for assessment of therapy and diagnosis in Parkinson's disease. Mov Disord 24: S725-S731.

126. Park EJ, Zhang YZ, Vykhodtseva N, McDannold N (2012) Ultrasound-mediated blood□brain/blood-tumor barrier disruption improves outcomes with trastuzumab in a breast cancer brain metastasis model. J Control Release 163: 277-284.

127. Alkins R, Burgess A, Kerbel R, Wels WS, Hynynen K (2016) Early treatment of HER2-amplified brain tumors with targeted NK-92 cells and focused ultrasound improves survival. Neuro Oncol 18: 974-981.

128. Chen PY, Hsieh HY, Huang CY, Lin CY, Wei KC, et al. (2015) Focused ultrasound-induced blood-brain barrier opening to enhance interleukin-12 delivery for brain tumor immunotherapy: A preclinical feasibility study. J Transl Med 13: 93.

129. Fan CH, Chang EL, Ting CY, Lin YC, Liao EC, et al. (2016) Folate-conjugated gene-carrying microbubbles with focused ultrasound for concurrent blood-brain barrier opening and local gene delivery. Biomaterials 106: 46-57.

130. Chang EL, Ting CY, Hsu PH, Lin YC, Liao EC, et al. (2017) Angiogenesis-targeting microbubbles combined with ultrasound-mediated gene therapy in brain tumors. J

Control Release 255: 164-175.

131. Zhou XL, Shi YL, Li X (2014) Inhibitory effects of the ultrasound-targeted microbubble destruction-mediated herpes simplex virus-thymidine kinase/ganciclovir system on ovarian cancer in mice. Exp Ther Med 8: 1159-1163.